Electronic Supporting Information (ESI) for:

Layered methylhydrazinium lead halide perovskites: new crystal polymorphs with tailored band gap and photoluminescence emission colour via halide substitution

Authors: Dawid Drozdowski,*[,a] Adam Kabański,[a] Dagmara Stefańska,[a] Maciej Ptak,[a]

Mirosław Mączka[a] and Anna Gągor*[,a]

[a]*Institute of Low Temperature and Structure Research, Polish Academy of Sciences, ul. Okólna 2, 50-422 Wrocław, Poland*

* - Corresponding Authors; e-mails: d.drozdowski@intibs.pl, a.gagor@intibs.pl

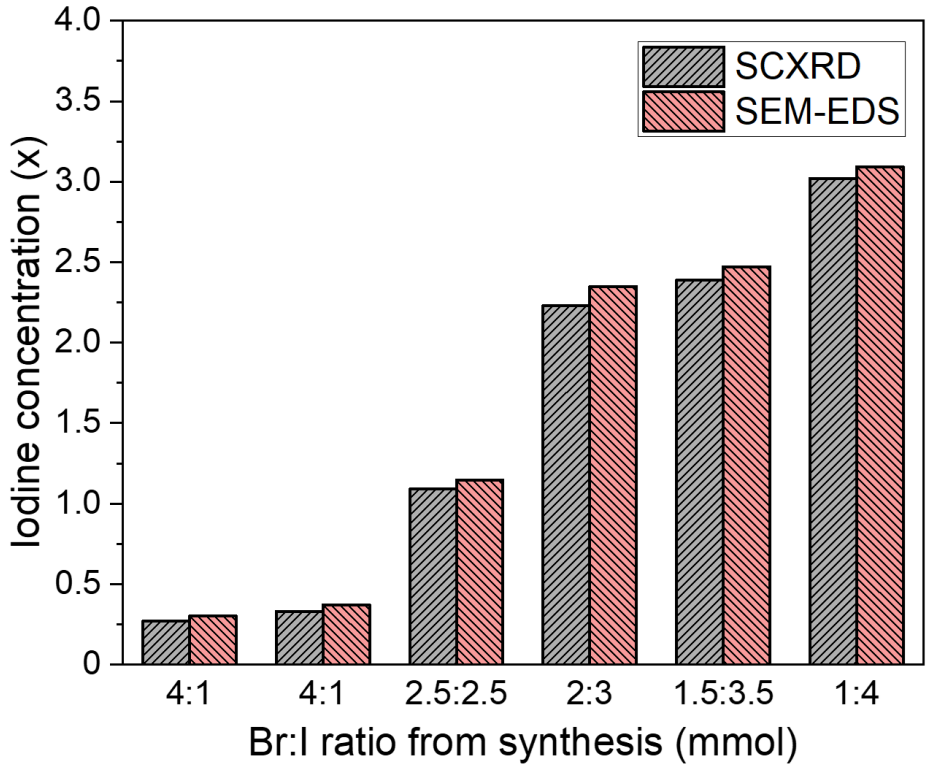

Figure S1. Comparison of the iodine contribution (*x*) calculated via elemental analysis (Scanning Electron Microscope with Energy Dispersive Spectrometer – SEM-EDS) and refined based on single-crystal X-ray diffraction data (site occupancy factors of halides refined as free parameters).

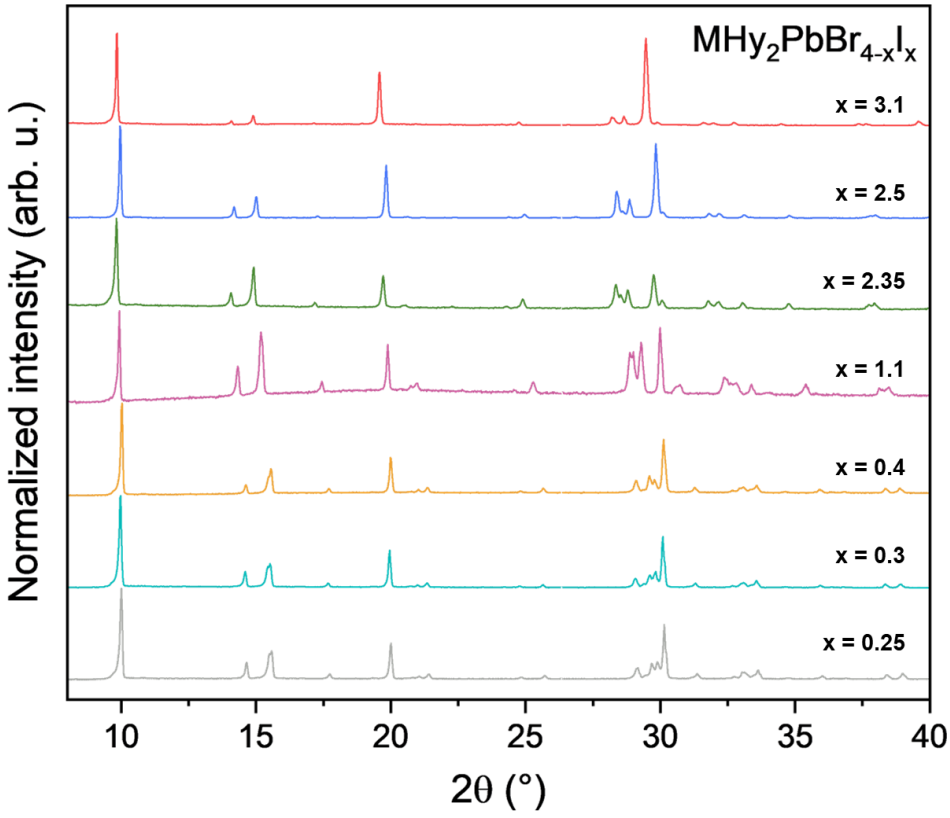

Figure S2. Powder X-ray diffraction patterns for $MHy_2PbBr_{4-x}I_x$ at 295 K testifying phase purity.

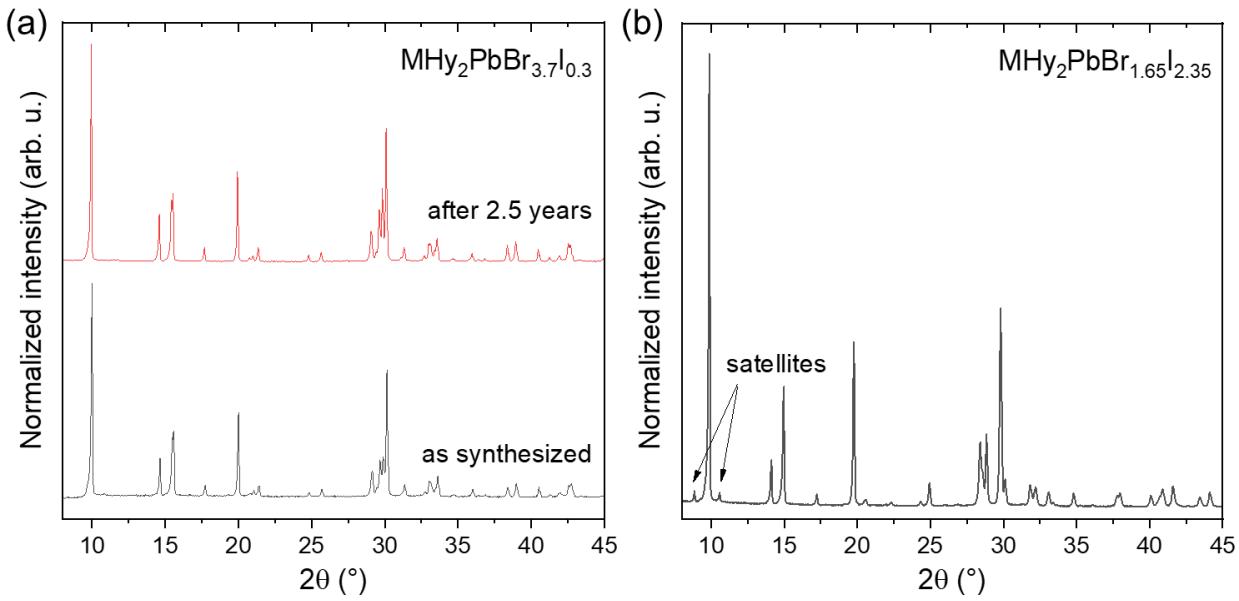

Figure S3. (a) The comparison of PXRD patterns for $MHyPbBr_{3.7}I_{0.3}$ (as-synthesized sample and stored *ca.* 2.5 years in a desiccator, RT) and (b) patterns for $MHyPbBr_{1.65}I_{2.35}$ (stored *ca.* 2.5 years in a desiccator, RT).

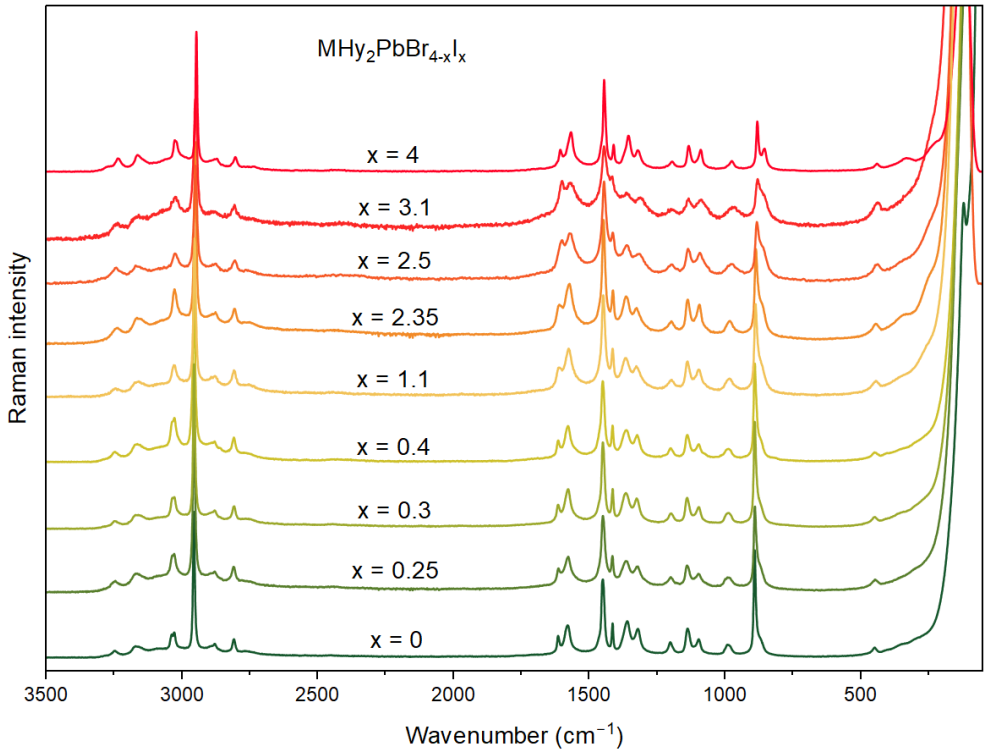

Figure S4. Raman spectra of polycrystalline $MHy_2PbBr_{4-x}I_x$ samples.

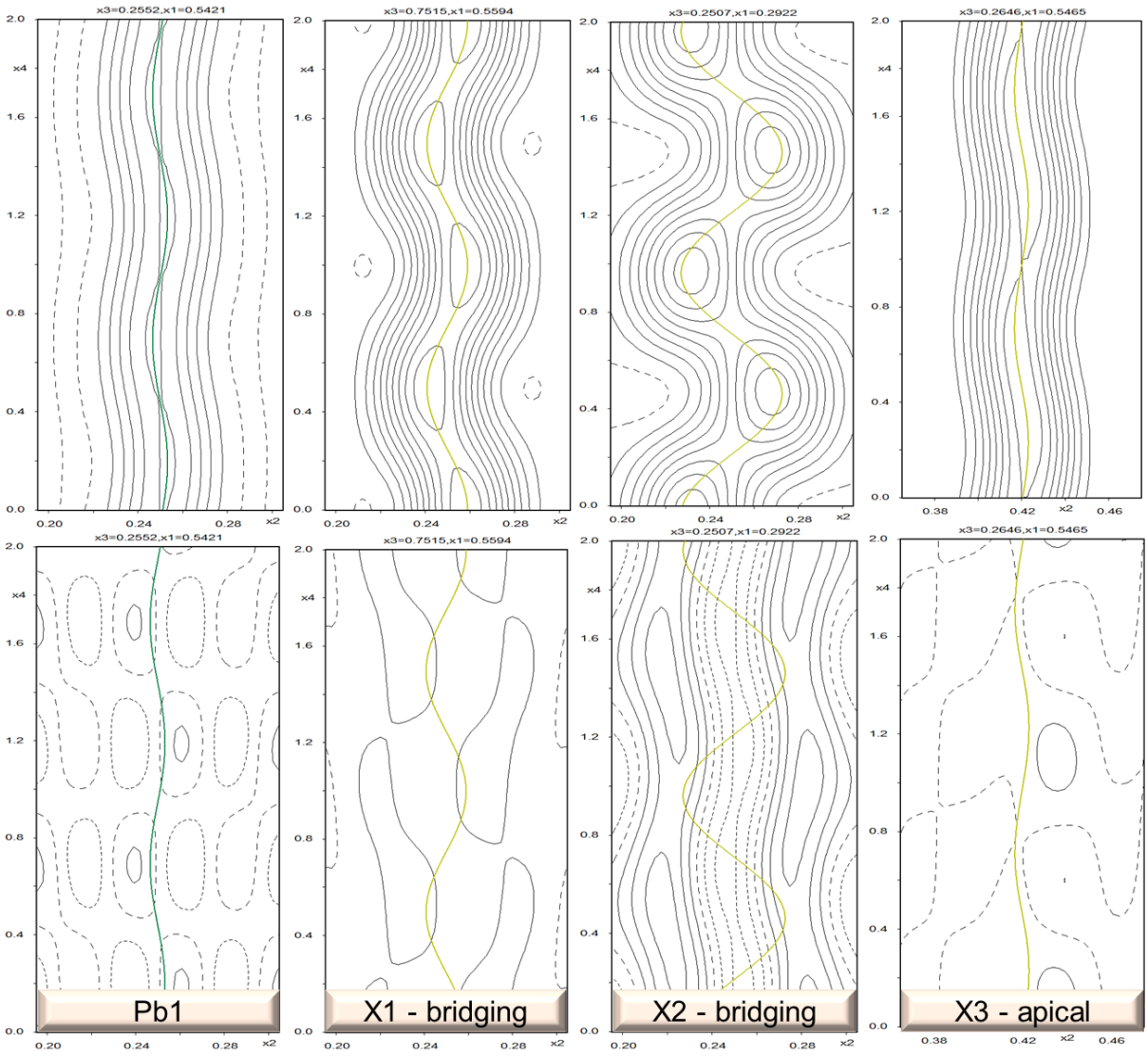

Figure S5. The x1-x4 sections through Pb and three inequivalent X atoms (X = Br, I) in $MHy_2PbBr_{0.9}I_{3.1}$ in modulated phase **VI**. Upper part: observed Fourier maps with contour step of 20 eÅ^{-3} for Pb and 5 eÅ^{-3} for X. Lower part: difference maps with the contour step of 0.5 eÅ^{-3} for all atoms. The dashed lines represent negative densities.

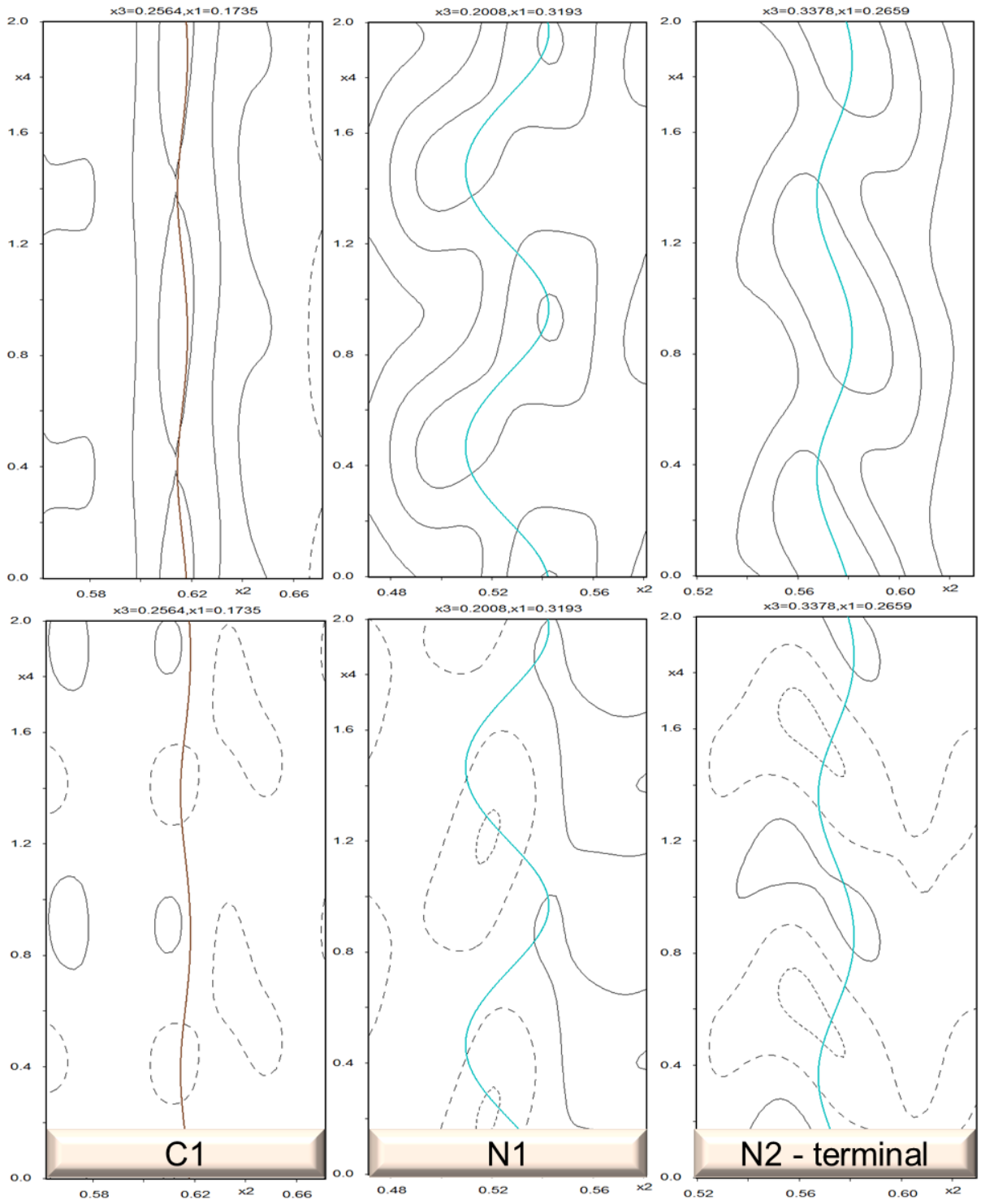

Figure S6. The x1-x4 sections through the atoms of MHy^{+} in $MHy_2PbBr_{0.9}I_{3.1}$ in modulated phase **VI**. Upper part: observed Fourier maps with contour step of 1 eÅ^{-3} for all atoms. Lower part: difference maps with the contour step of 0.5 eÅ^{-3} for all atoms. The dashed lines represent negative densities.

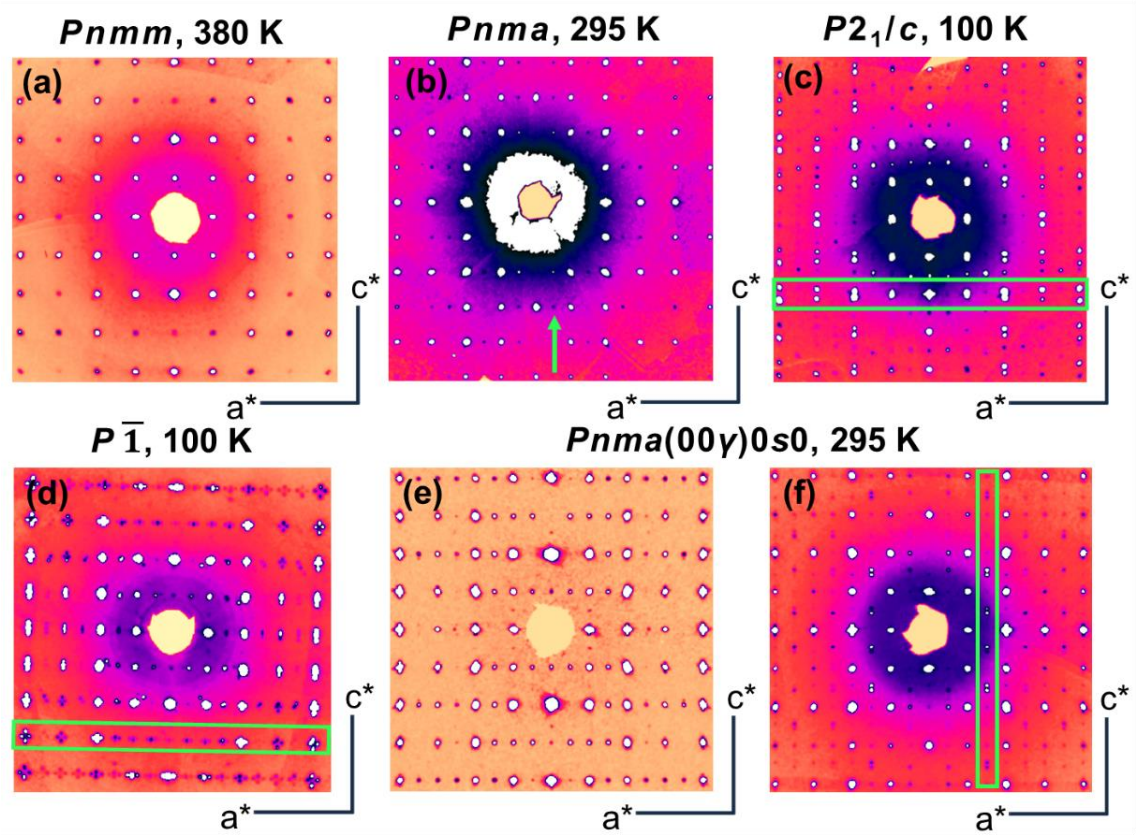

Figure S7. Reciprocal space reconstruction of the (a-d) *h*0*l* layer in particular phases: (a, b, c) *Pnmm*, *Pnma* and $P2_1/c$ (**II**, **III** and **IV**, respectively), (d) $P\bar{1}$ (**V**). (e-f) To apply the systematic extinctions rule for satellite reflections in modulated phase, four integers *hklm* (ha* + kb* + lc* + mq) are provided to index all peaks. For (e) *h*0*lm* layer, the 1st order satellite reflections (m = 1) do not appear, while for (f) *h*1*lm* layer are visible. According to the *International Tables for Crystallography Volume C* (Janssen *et al.*, 2006) this rule applies to an intrinsic shift s along the [010] direction. Therefore, the (3+1)-dimensional superspace group is *Pnma*(00*γ*)0*s*0 (**VI**).

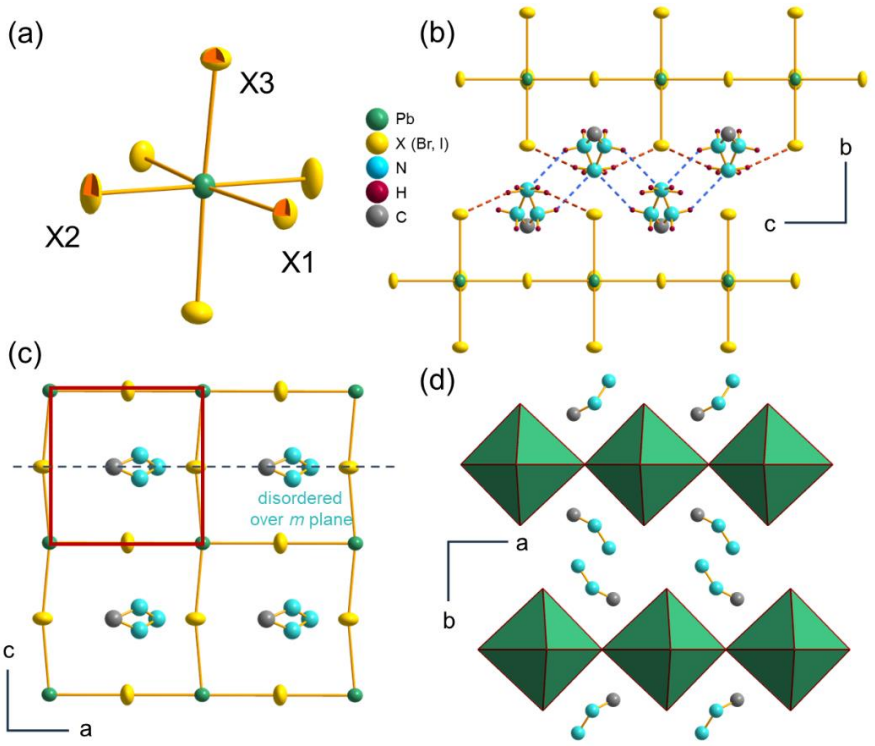

Figure S8. Crystal structure of $MHy_2PbBr_{3.7}I_{0.3}$ (1st region) in **II** at 380 K. (a) Individual octahedra with three independent halides. View along (b) [100], (c) [010] and (d) [001] direction. Dashed lines in (b) represent possible hydrogen bonding (HBs) interactions.

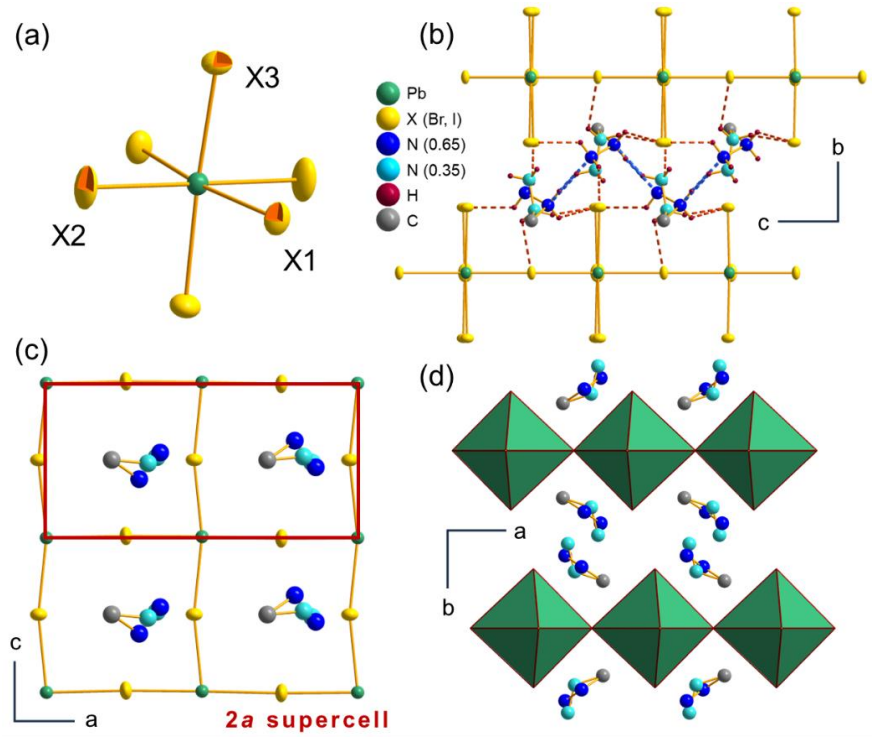

Figure S9. Crystal structure of $MHy_2PbBr_{3.7}I_{0.3}$ (1st region) in **III** at 295 K. (a) Individual octahedra with three independent halides. View along (b) [100], (c) [010] and (d) [001] direction. Dashed lines in (b) represent possible HBs.

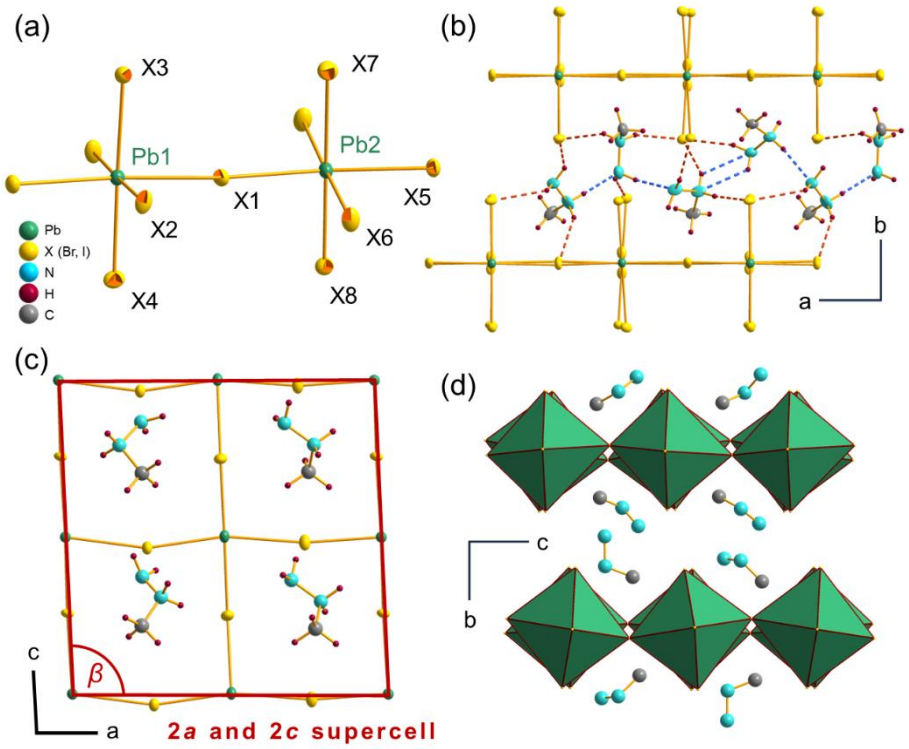

Figure S10. Crystal structure of $MHy_2PbBr_{3.7}I_{0.3}$ (1^{st} region) in **IV** at 100 K. (a) Two $[PbX_6]^{4-}$ octahedra in the assymetric unit. View along (b) [001], (c) [010] and (d) [100] direction. Dashed lines in (b) represent possible HBs.

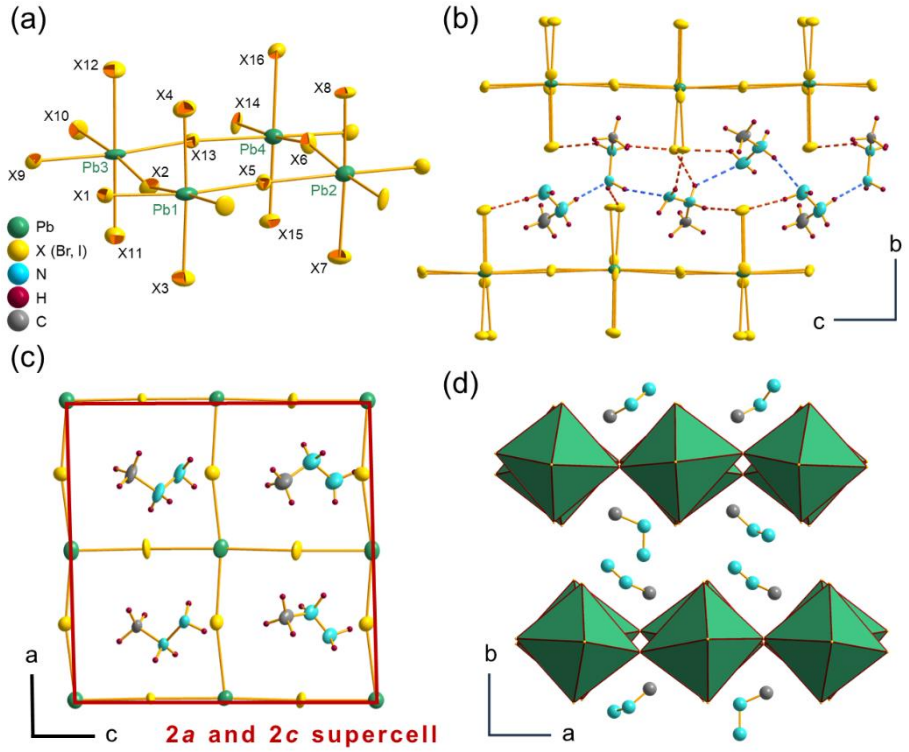

Figure S11. Crystal structure of $MHy_2PbBr_{2.9}I_{1.1}$ (2^{nd} region) in **V** at 100 K. (a) Four $[PbX_6]^{4-}$ octahedra in the assymetric unit. View along (b) [100], (c) [010] and (d) [001] direction. Dashed lines in (b) represent possible HBs.

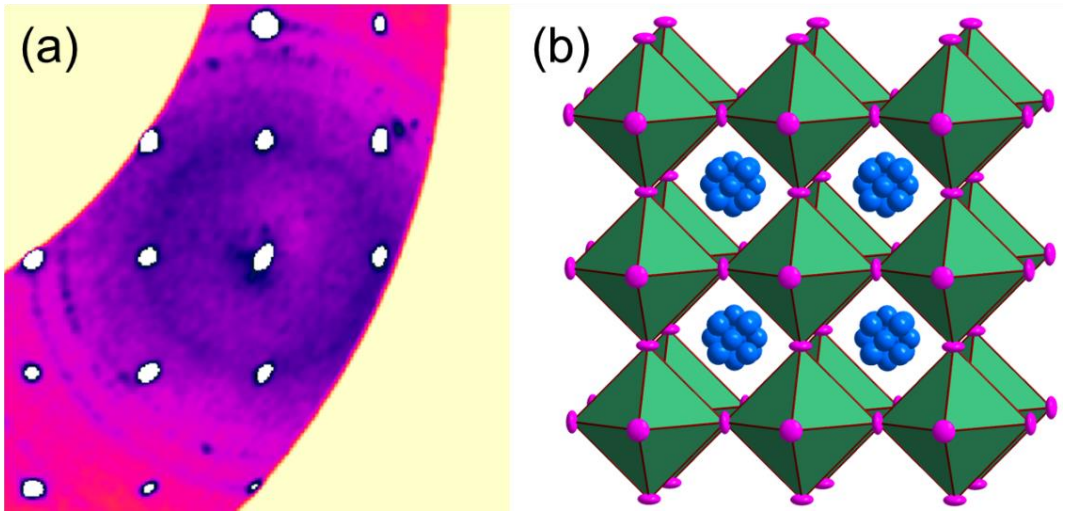

Figure S12. (a) Reciprocal space reconstruction and (b) crystal structure of $MHy_2PbBr_{1.5}I_{2.5}$ in $Pm\bar{3}m$ (**I**) at 350 K. Measured after pre-heating to 370 K.

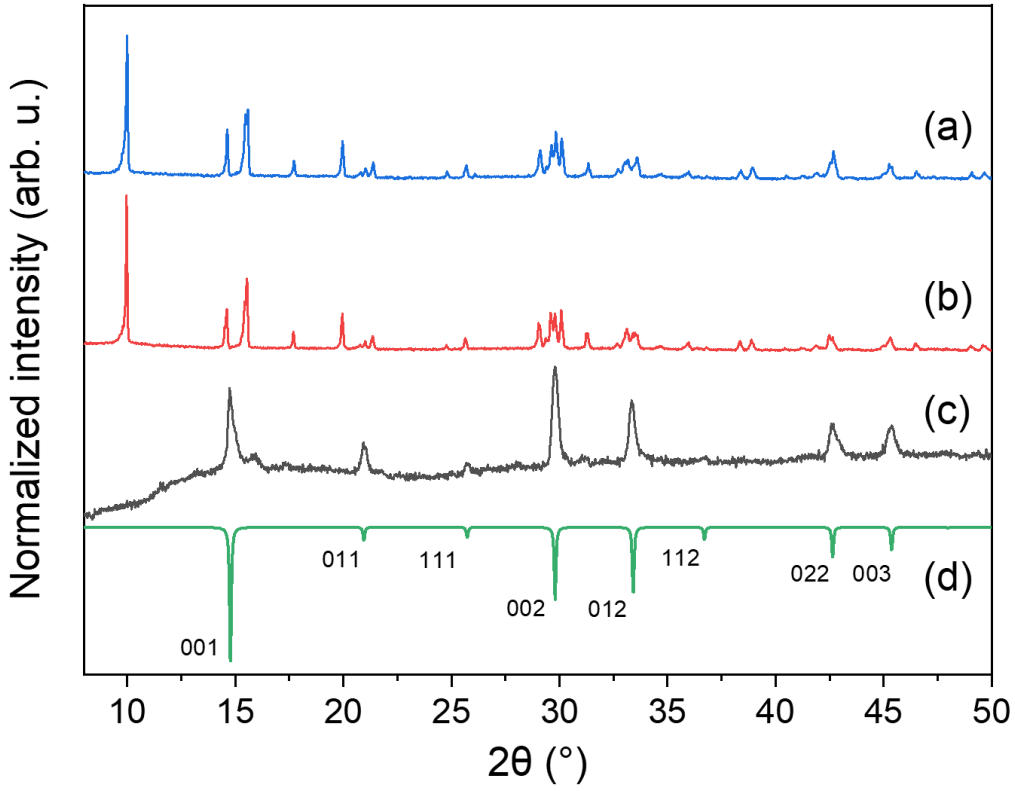

Figure S13. (a-c) Experimental powder XRD diffractograms of $MHy_2PbBr_{3.7}I_{0.3}$ (a) at RT (*Pnma*, **III**), (b) at RT after heating at 375 K (**III**), (c) at RT after heating at 420 K ($Pm\bar{3}m$, **I**). (d) Theoretical diffractogram for phase **I** with a = 5.992(3) Å.

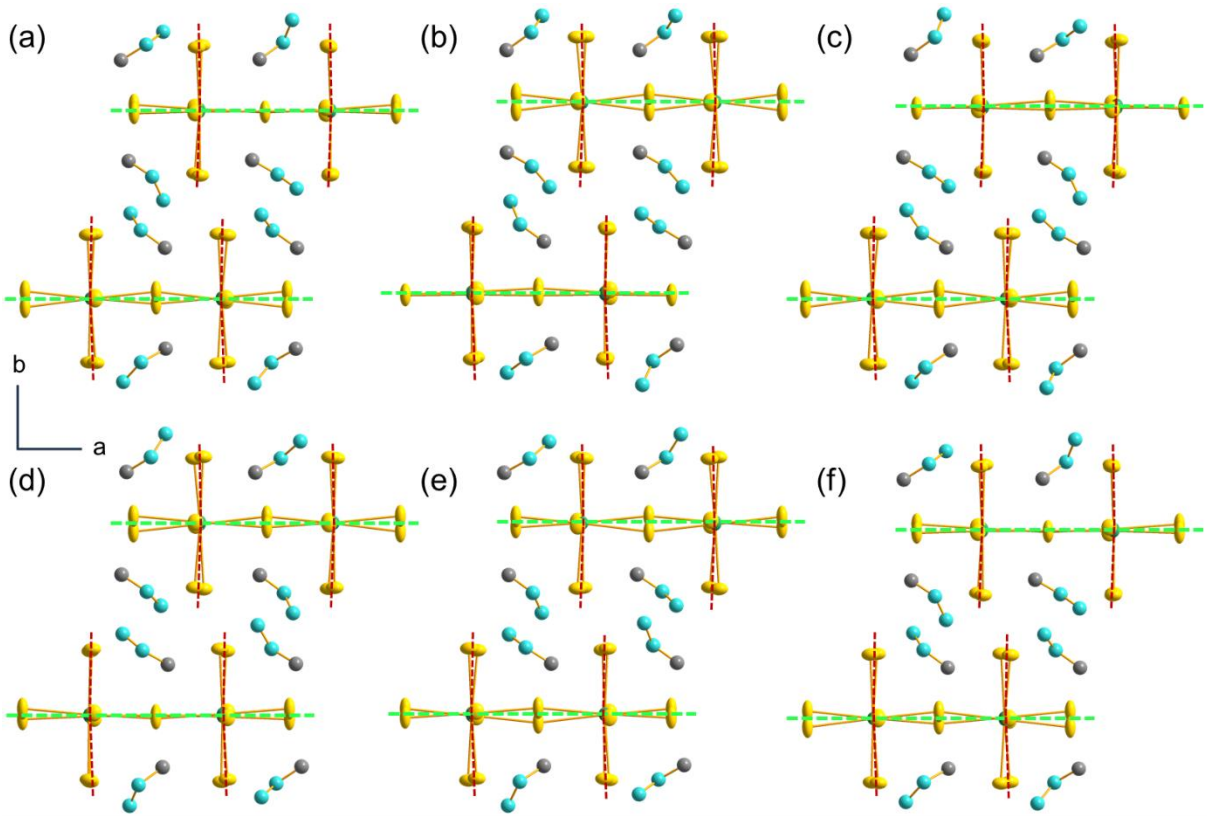

Figure S14. Snapshots of the modulation in phase **VI** in $MHy_2PbBr_{0.9}I_{3.1}$ at 295 K for *t* values equal to (a) 0, (b) 0.2, (c) 0.4, (d) 0.6, (e) 0.8 and (f) 1.0 Dashed lines represent coordinates of X1 (green) and X3 (red) in the averaged structure.

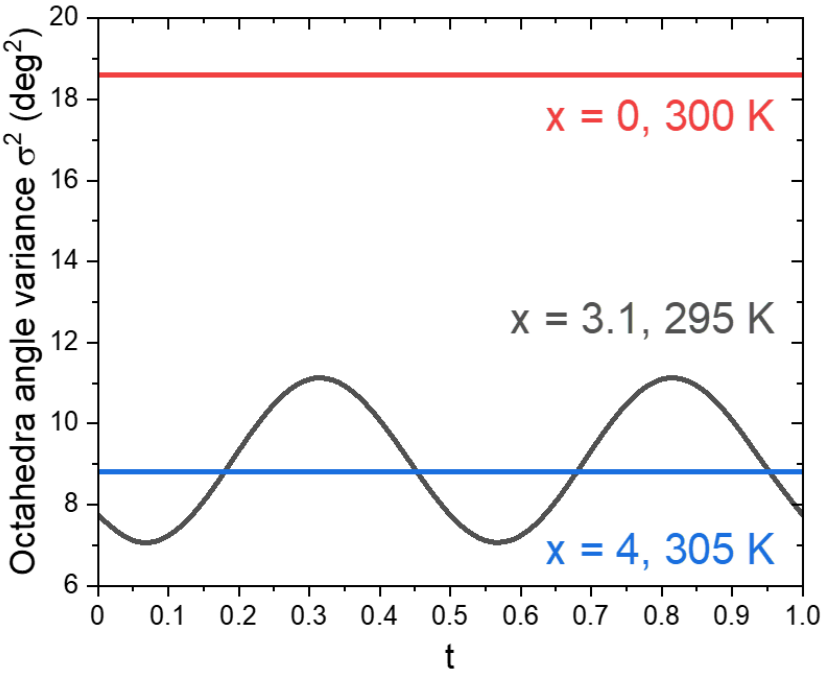

Figure S15. Octahedra angle variance σ^2 of $MHy_2PbBr_{0.9}I_{3.1}$ in modulated phase (**VI**) at 295 K versus *t*, compared with single halide analogues – MHy_2PbBr_4 (*Pmn*2_1, 300 K) and MHy_2PbI_4 (*Pmmn*, 305 K).

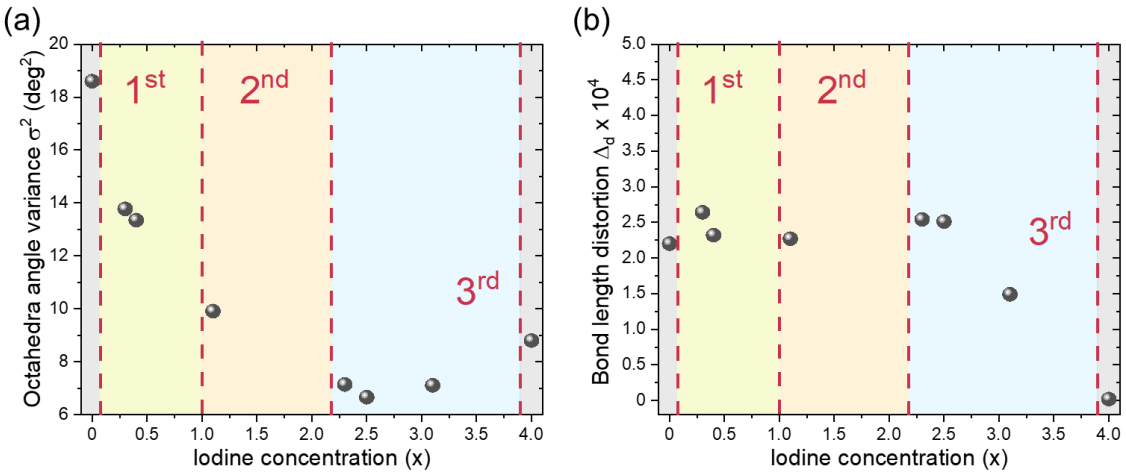

Figure S16. Octahedra distortion parameters of $MHy_2PbBr_{4-x}I_x$ versus iodine concentration (x): (a) bond length distortion (Δ_d) and (b) octahedra angle variance (σ^2). Values for the samples in the 3rd region are provided for the averaged structure of **VI**.

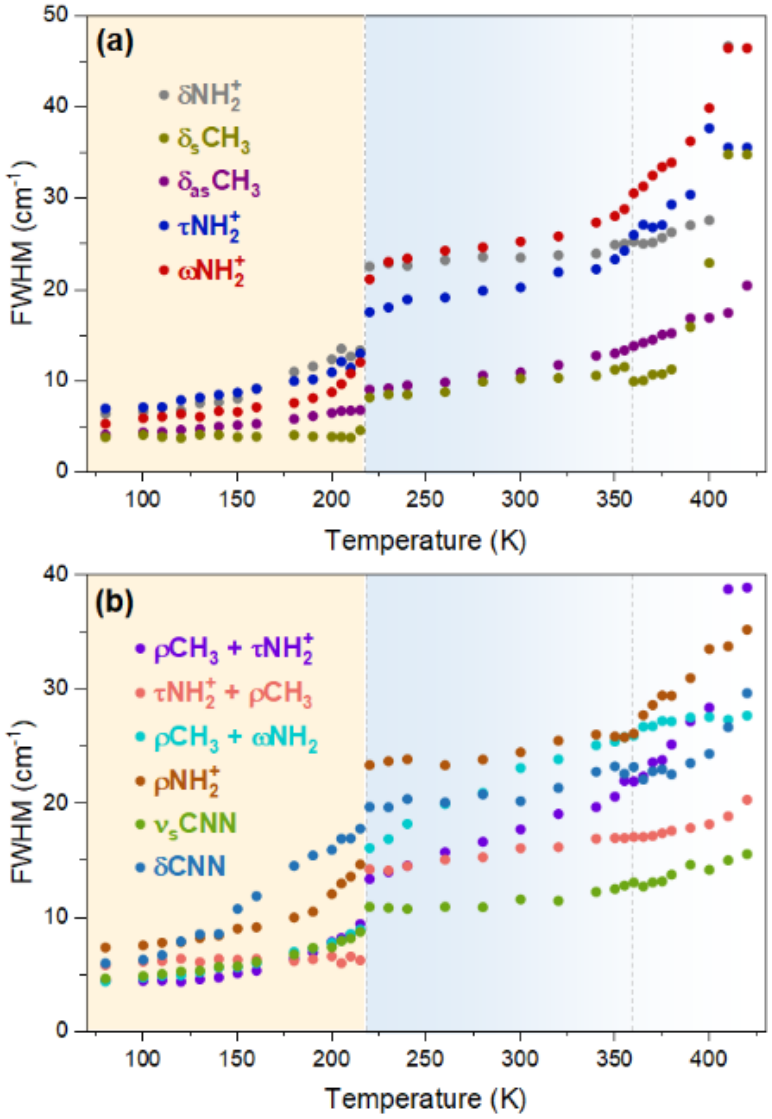

Figure S17. Dependences of FWHMs of selected Raman bands as a function of temperature for the $MHy_2PbBr_{3.7}I_{0.3}$ sample.

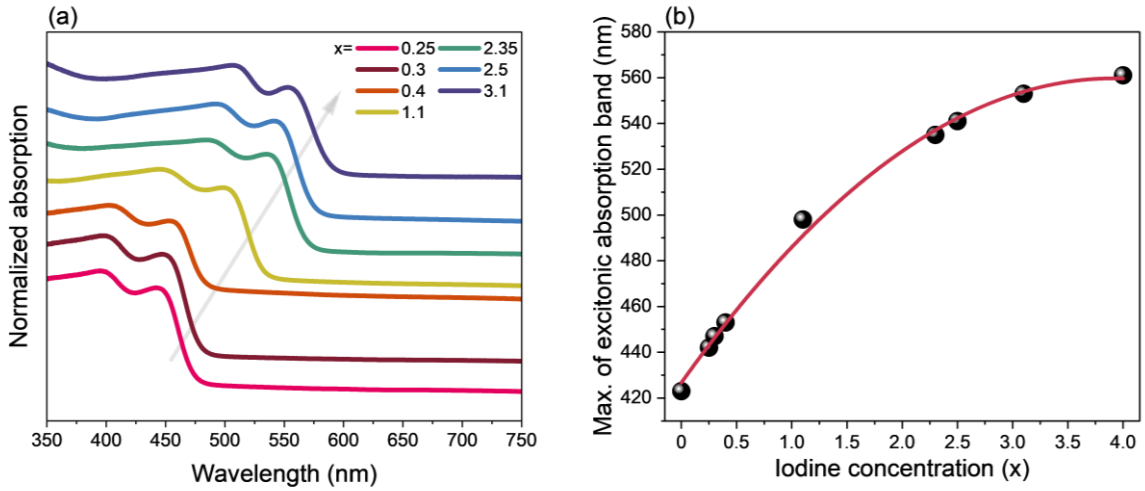

Figure S18. (a) Room temperature absorption spectra and (b) position of the maximum of the excitonic absorption band consolidated with the 2nd-order polynomial fitting (red curve) of the investigated samples of $MHy_2PbBr_{4-x}I_x$.

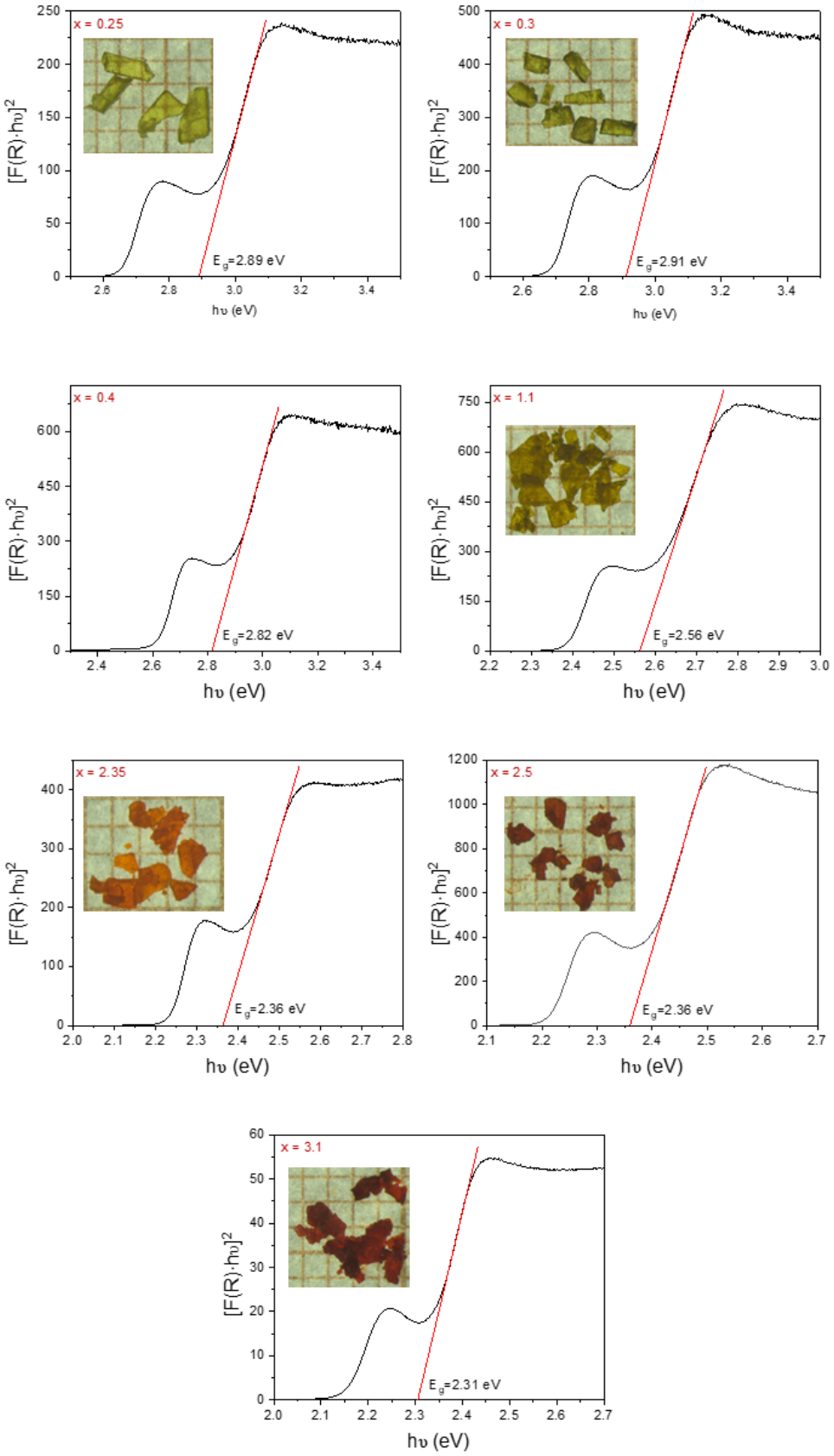

Figure S19. The energy of band gaps determined with Tauc plots for investigated materials of $MHy_2PbBr_{4-x}I_x$. The composition of the individual material is presented in the plot. The insets represent the actual samples, placed on a graph paper (1 grid = 1 mm).

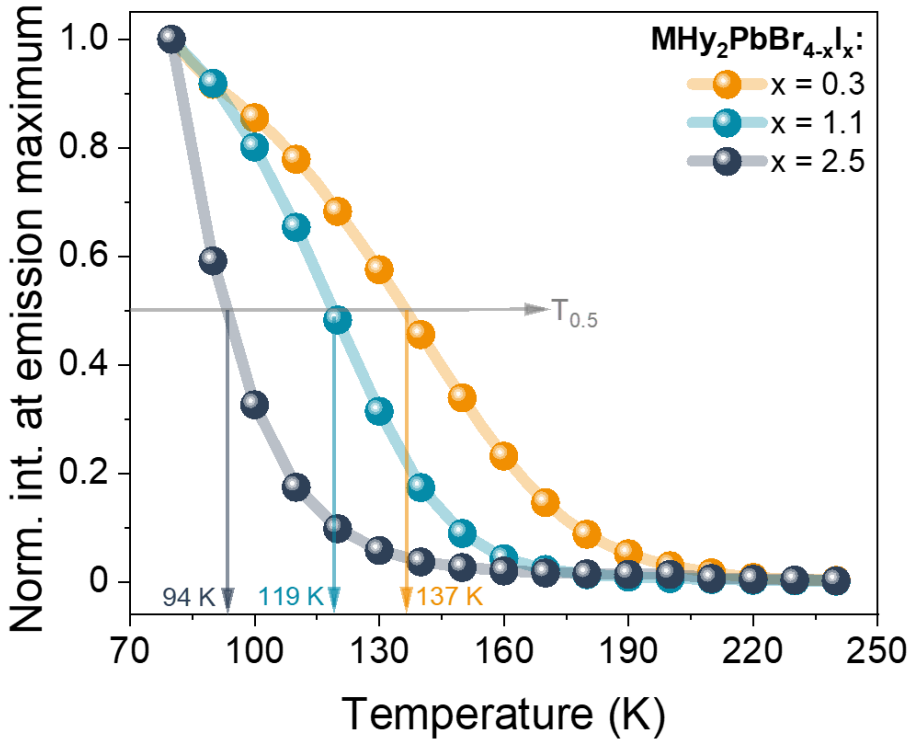

Figure S20. The influence of temperature on normalized integrated PL intensities.

Table S1. Experimental and refinement details of $MHy_2PbBr_{3.7}I_{0.3}$ (M_r = 635.08).

	Phase II	**Phase III**	**Phase IV**
Crystal data			
Crystal system, space group	Orthorhombic, *Pnmm*	Orthorhombic, *Pnma*	Monoclinic, $P2_1/c$
Temperature (K)	380	295	100
a, *b*, *c* (Å)	6.097(3), 18.194(3), 6.063(5)	12.205(4), 17.858(5), 6.054(3)	12.120(4), 17.609(5), 12.099(3)
β (°)	90, 90, 90	90, 90, 90	90, 92.52(3), 90
V (Å^3)	672.5(7)	1319.7(9)	2579.6(13)
Z	2	4	8
μ (mm^{-1})	24.18	24.68	25.25
Crystal size (mm)	0.16 × 0.12 × 0.03	0.16 × 0.12 × 0.03	0.16 × 0.12 × 0.03
Data collection			
T_{min}, T_{max}	0.109, 1.000	0.240, 1.000	0.240, 1.000
No. of measured, independent and observed [$I > 2\sigma(I)$] reflections	14587, 735, 702	20001, 1394, 940	8313, 8313, 4120
R_{int}	0.044	0.042	-
$(\sin \theta/\lambda)_{max}$ (Å^{-1})	0.609	0.625	0.610
Refinement			
$R[F^2 > 2\sigma(F^2)]$, $wR(F^2)$, S	0.034, 0.097, 1.24	0.026, 0.069, 1.05	0.048, 0.126, 0.89
No. of reflections	735	1394	8313
No. of parameters	40	60	160
No. of restraints	0	2	1
$\Delta\rho_{max}$, $\Delta\rho_{min}$ (e Å^{-3})	1.62, -1.35	0.63, -0.86	2.86, -2.67

Table S2. Experimental and refinement details of $MHy_2PbBr_{2.9}I_{1.1}$ (M_r = 672.68).

	Phase III	**Phase V**
Crystal data		
Crystal system, space group	Orthorhombic, *Pnma*	Triclinic, *P*-1
Temperature (K)	295	100
a, *b*, *c* (Å)	12.391(4), 17.892(5), 6.166(3)	12.318(4), 17.655(5), 12.297(4)
β (°)	90, 90, 90	90.04(3), 88.85(3), 89.98(3)
V (Å^3)	1366.9(9)	2673.6(14)
Z	4	8
μ (mm^{-1})	23.27	23.92
Crystal size (mm)	0.28 × 0.18 × 0.07	0.28 × 0.18 × 0.07
Data collection		
T_{min}, T_{max}	0.346, 1.000	0.159, 1.000
No. of measured, independent and observed [$I > 2\sigma(I)$] reflections	8147, 1444, 846	11196, 11196, 5598
R_{int}	0.040	-
$(\sin \theta/\lambda)_{max}$ (Å^{-1})	0.625	0.610
Refinement		
$R[F^2 > 2\sigma(F^2)]$, $wR(F^2)$, S	0.032, 0.073, 1.03	0.107, 0.314, 1.01
No. of reflections	1444	11196
No. of parameters	61	318
No. of restraints	2	85
$\Delta\rho_{max}$, $\Delta\rho_{min}$ (e Å^{-3})	0.86, -1.52	12.55, -5.90

Table S3. Experimental and refinement details of compounds crystallizing in modulated phase (**VI**): $MHy_2PbBr_{1.65}I_{2.35}$ (M_r = 731.43), $MHy_2PbBr_{1.5}I_{2.5}$ (M_r = 738.48), $MHy_2PbBr_{0.9}I_{3.1}$ (M_r = 766.68) and for $MHy_2PbBr_{1.5}I_{2.5}$ in phase **I**. For the first two compounds values are provided for averaged structures.

	$MHy_2PbBr_{1.65}I_{2.35}$	**$MHy_2PbBr_{1.5}I_{2.5}$**	**$MHy_2PbBr_{0.9}I_{3.1}$**	**$MHy_2PbBr_{1.5}I_{2.5}$**
Crystal data				
Crystal system, space group	Orthorhombic, *Pnma*(00γ)*s*00			Cubic, *Pm*-3*m*
Modulation vector, *q*	0.456**c***	0.454**c***	0.440**c***	-
Temperature (K)	295			350
a, *b*, *c* (Å)	12.600(4), 18.024(5), 6.303(3)	12.642(4), 18.070(5), 6.330(3)	12.710(4), 18.271(5), 6.363(3)	6.270(3)
V (Å^3)	1431.5(9)	1319.7(9)	1477.7(9)	246.4(4)
Z	4			1
μ (mm^{-1})	21.50	21.18	20.30	26.43
Crystal size (mm)	0.2 × 0.08 × 0.03	0.25 × 0.13 × 0.03	0.3 × 0.14 × 0.07	0.25 × 0.13 × 0.03
Data collection				
T_{min}, T_{max}	0.294, 1.000	0.187, 1.000	0.473, 1.000	0.418, 1.000
No. of measured, independent and observed reflections	27011, 1509, 1101	54228, 1523, 1111	183735, 5912, 2458	551, 76, 63
R_{int}	0.038	0.049	0.060	0.053
(sin θ/λ)$_{max}$ (Å^{-1})	0.624	0.625	0.695	0.623
Refinement				
$R[F^2 > 2\sigma(F^2)]$, $wR(F^2)$, *S* (all)	0.041, 0.124, 1.10	0.047, 0.146, 1.13	0.059, 0.222, 2.32	0.050, 0.123, 1.08
$R[F^2 > 2\sigma(F^2)]$, $wR(F^2)$ (main)	-	-	0.039, 0.124	-
$R[F^2 > 2\sigma(F^2)]$, $wR(F^2)$ (satellites)	-	-	0.128, 0.286	-
No. of reflections	1509	1523	5912	76
No. of parameters	48	48	58	8
No. of restraints	4	4	2	-
$\Delta\rho_{max}$, $\Delta\rho_{min}$ (e Å^{-3})	2.42, -2.86	2.89, -3.25	1.93, -2.02	0.83, -0.54

Table S4. Selected hydrogen-bond parameters of $MHy_2PbBr_{3.7}I_{0.3}$.

D—H···*A*	*D*—H (Å)	H···*A* (Å)	*D*···*A* (Å)	*D*—H···*A* (°)
Phase III, 295 K				
N3A—H3AA···Br3^{i}	0.89	2.61	3.316 (11)	136.7
N3A—H3AB···Br3	0.89	2.76	3.534 (15)	146.0
N2A—H2AA···Br3^{ii}	0.89	2.63	3.289 (9)	131.4
N2A—H2AB···N3A^{iii}	0.89	2.23	3.110 (17)	170.9
N2—H2A···Br1^{ii}	0.89	2.82	3.41 (3)	125.1
N2—H2B···Br3^{ii}	0.89	2.73	3.531 (17)	150.7
N3—H3A···N3^{iii}	0.90	2.56	3.335 (19)	144.4
N3—H3B···N3^{iv}	0.90	2.49	3.335 (19)	157.1
Phase IV, 100 K				
N6—H6A···Br1^{v}	0.92	2.91	3.736 (17)	150.4
N6—H6B···Br8^{vi}	0.93	2.58	3.497 (17)	169.9
N8—H8A···Br3^{i}	0.89	2.86	3.501 (15)	129.6
N8—H8B···Br7	0.89	2.68	3.451 (16)	146.1
N4—H4D···Br7^{i}	0.91	2.72	3.530 (16)	149.4
N4—H4E···N6	0.91	2.26	3.13 (2)	159.5
N3—H3D···Br7	0.91	2.50	3.357 (15)	157.6
N3—H3E···Br3	0.91	2.47	3.292 (16)	151.0
N1—H1A···N4	0.91	1.98	2.890 (19)	177.9
N1—H1B···Br5^{v}	0.91	2.73	3.514 (17)	144.6
N1—H1B···Br8^{v}	0.91	2.93	3.407 (14)	114.6
N5—H5A···Br7	0.91	2.56	3.325 (17)	142.5
N5—H5A···N8	0.91	2.57	3.21 (2)	127.9
N5—H5B···Br4^{v}	0.91	2.45	3.321 (16)	161.5
N7—H7A···N2^{vii}	0.91	2.14	3.04 (2)	168.9
N7—H7B···Br2^{vii}	0.91	2.89	3.549 (17)	130.6
N7—H7B···Br3^{vii}	0.91	2.85	3.396 (14)	120.0
N2—H2D···Br4^{vi}	0.88	2.74	3.409 (16)	133.4
N2—H2E···Br4^{viii}	0.88	2.53	3.395 (15)	165.2

Symmetry code(s): (i) -*x*+1, -*y*+1, -*z*; (ii) -*x*+1, -*y*+1, -*z*+1; (iii) -*x*+1/2, -*y*+1, *z*+1/2; (iv) -*x*+1/2, -*y*+1, *z*-1/2; (v) -*x*+1, *y*+1/2, -*z*+1/2; (vi) *x*, -*y*+1/2, *z*+1/2; (vii) *x*+1, *y*, *z*; (viii) -*x*, *y*+1/2, -*z*+1/2.

Table S5. Selected hydrogen-bond parameters of $MHy_2PbBr_{2.9}I_{1.1}$.

D—H···*A*	*D*—H (Å)	H···*A* (Å)	*D*···*A* (Å)	*D*—H···*A* (°)
Phase III, 295 K				
N3A—H3AA···Br3^{i}	0.90	2.66	3.329 (12)	132.0
N3A—H3AB···Br3	0.90	2.77	3.604 (18)	154.4
N2A—H2AA···Br3^{ii}	0.89	2.61	3.309 (11)	136.2
N2A—H2AB···N3A^{iii}	0.89	2.24	3.105 (18)	165.7
N3—H3B···Br3^{iv}	0.89	2.78	3.62 (3)	159.8
N2—H2A···Br1^{ii}	0.89	2.82	3.43 (3)	127.2
N2—H2B···Br3^{ii}	0.89	2.71	3.52 (2)	151.7
Phase V, 100 K				
N24—H24A···Br9^{ii}	0.90	2.74	3.52 (3)	144.3
N24—H24B···Br15	0.91	2.65	3.44 (4)	145.3
N11—H11A···Br16	0.91	2.63	3.46 (4)	151.3
N11—H11B···Br10	0.91	2.49	3.38 (4)	164.5
N6—H6A···N8^{v}	0.90	2.49	3.24 (5)	141.7
N6—H6B···Br10	0.90	2.76	3.58 (4)	152.5
N15—H15B···Br4^{vi}	0.90	2.73	3.52 (4)	147.2
N8—H8A···Br10^{v}	0.91	2.79	3.46 (4)	130.9
N8—H8A···N6^{v}	0.91	2.53	3.24 (5)	135.2
N8—H8B···Br12	0.91	2.47	3.33 (4)	159.0
N23—H23A···Br9	0.91	2.82	3.35 (3)	118.5
N23—H23B···N21^{ii}	0.91	2.14	3.05 (6)	176.0
N18—H18A···N15^{i}	0.89	2.32	3.15 (6)	155.5
N18—H18B···Br15^{ii}	0.89	2.62	3.51 (5)	172.0
N17—H17A···Br15^{vii}	0.91	2.44	3.32 (3)	162.8
N17—H17B···Br9	0.91	2.77	3.57 (5)	147.3
N2—H2A···N12^{v}	0.91	2.10	3.00 (6)	172.6
N2—H2B···Br3	0.91	2.74	3.58 (4)	155.0
N9—H9A···Br13^{viii}	0.90	2.58	3.48 (4)	170.5
N5—H5A···Br16^{vii}	0.91	2.91	3.42 (3)	116.6
N5—H5B···N3^{ix}	0.91	2.20	3.10 (5)	169.7
N20—H20A···N18^{ii}	0.91	2.03	2.93 (6)	174.1
N20—H20B···Br17	0.91	2.78	3.60 (4)	150.1
N12—H12A···N9^{v}	0.92	2.40	3.29 (6)	163.9
N12—H12B···Br10^{v}	0.92	2.62	3.52 (3)	166.6
N14—H14A···Br15^{ii}	0.91	2.73	3.43 (4)	134.9
N14—H14A···N24^{ii}	0.91	2.37	3.10 (5)	137.0
N14—H14B···Br1	0.91	2.51	3.38 (4)	161.5
N21—H21A···Br1	0.91	2.52	3.42 (5)	170.1
N21—H21B···Br1^{vi}	0.90	2.69	3.41 (4)	138.3

Symmetry code(s): (i) -*x*+1, -*y*+1, -*z*; (ii) -*x*+1, -*y*+1, -*z*+1; (iii) -*x*+1/2, -*y*+1, *z*+1/2; (iv) *x*-1/2, *y*, -*z*+1/2; (v) -*x*+1, -*y*, -*z*+1; (vi) -*x*, -*y*+1, -*z*+1; (vii) *x*, *y*, *z*-1; (viii) -*x*, -*y*, -*z*+1; (ix) -*x*+1, -*y*, -*z*.

Table S6. Raman wavenumbers for polycrystalline $MHy_2PbBr_{4-x}I_x$ samples, together with band assignments.[a]

4	3.1	2.5	2.35	1.1	0.4	0.3	0.25	0	Assignment
3270_{vw}					3283_{vw}		3278_{vw}	3279_{vw}	$\nu_{as}NH_2$
3235_{w}	3240_{w}	3243_{w}	3238_{w}	3244_{w}	3247_{w}	3248_{w}	3246_{w}	3247_{w}	$\nu_{s}NH_2$
3163_{w}	3160_{w}	3165_{w}	3159_{w}	3162_{w}	3164_{w}	3166_{w}	3168_{w}	3167_{w}	$\nu_{as}NH_2^+$
3078_{w}			3079_{w}	3085_{w}	3090_{w}	3091_{w}	3089_{w}	3087_{w}	$\nu_{s}NH_2^+$
3025_{w}	3025_{w}	3025_{w}	3026_{w}	3028_{w}	3036_{w}, 3028_{w}	3036_{w}, 3029_{w}	3036_{w}, 3029_{w}	3038_{w}, 3029_{w}	$\nu_{as}CH_3$
2948_{s}	2953_{s}	2951_{s}	2952_{s}	2954_{s}	2957_{s}	2956_{s}	2955_{s}	2955_{s}	$\nu_{s}CH_3$
2876_{vw}, 2805_{w}	2883_{vw}, 2808_{w}	2882_{vw}, 2806_{w}	2878_{vw}, 2807_{w}	2880_{vw}, 2809_{w}	2881_{vw}, 2809_{w}	2880_{vw}, 2809_{w}	2880_{vw}, 2809_{w}	2880_{vw}, 2809_{w}	overtone
1607_{w}	1601_{w}	1602_{w}	1611_{w}	1609_{w}	1615_{w}	1617_{vw}	1614_{w}	1615_{w}	δNH_2
1568_{m}	1572_{m}	1571_{m}	1575_{m}	1577_{m}	1579_{m}	1584_{m}	1579_{m}	1580_{m}	δNH_2^+
1446_{s}	1445_{s}	1446_{s}	1448_{s}	1448_{s}	1451_{s}	1452_{s}	1450_{s}	1451_{s}	$\delta_{as}CH_3$
1411_{w}	1417_{w}	1414_{w}	1414_{w}	1415_{w}	1415_{w}	1417_{vw}	1416_{w}	1414_{w}	$\delta_{s}CH_3$
1357_{m}	1364_{m}	1363_{m}	1364_{m}	1367_{m}	1365_{m}	1374_{w}	1365_{m}	1361_{m}	ωNH_2^+
1322_{m}	1313_{m}	1319_{m}	1328_{m}	1326_{m}	1325_{m}	1327_{m}	1324_{m}	1321_{m}	τNH_2^+
1196_{w}	1197_{w}	1198_{w}	1198_{w}	1200_{w}	1201_{w}	1203_{w}	1201_{w}	1202_{w}	$\rho CH_3+\omega NH_2$
1135_{m}	1135_{m}	1136_{m}	1139_{m}	1139_{m}	1140_{m}	1140_{m}	1140_{m}	1139_{m}	$\tau NH_2^+ + \rho CH_3$
1090_{w}	1090_{w}	1094_{w}	1096_{w}	1097_{w}	1098_{w}	1099_{m}	1098_{w}	1098_{w}	$\rho CH_3+\tau NH_2^+$
976_{w}	971_{w}	976_{w}	984_{w}	985_{w}	989_{w}	985_{w}	989_{w}	989_{w}	$\nu_{as}CNN$
882_{s}	880_{s}	883_{s}	887_{s}	888_{s}	891_{s}	894_{s}	891_{s}	892_{s}	$\nu_{s}CNN$
856_{sh}	866_{sh}	868_{sh}	871_{sh}	872_{sh}	872_{sh}	872_{sh}	873_{m}	872_{sh}	ρNH_2^+
441_{w}	439_{w}	441_{w}	446_{w}	444_{w}	449_{w}	451_{w}	448_{w}	450_{w}	δCNN
331_{w}		347_{w}	340_{w}	349_{w}	347_{w}	342_{w}		346_{w}	τNH_2
225_{vw}		241_{vw}	255_{vw}	259_{vw}	295_{vw}	285_{vw}	295_{vw}	295_{vw}	τCH_3
122_{s}	107_{s}	129_{s}	107_{s}	116_{s}	122_{s}	119_{s}	121_{s}	123_{s}	$\nu PbBr+T'+L$
	58_{vs}		57_{vs}	58_{vs}	57_{vs}		57_{vs}	56_{vs}	$\delta PbBr$

[a]key: δ, bending; ρ, rocking; ν, stretching; τ, twisting; ω, wagging; T', MHy^+ translation; L, MHy^+ vibration; vs, very strong; s, strong or symmetric; m, medium; w, weak; vw, very weak; as, antisymmetric.